

# Structural Basis of Ets1 Cooperative Binding to Widely Separated Sites on Promoter DNA

Nigar D. Babayeva, Oxana I. Baranovskaya, Tahir H. Tahirov\*

Eppley Institute for Research in Cancer and Allied Diseases, University of Nebraska Medical Center, Omaha, Nebraska, United States of America

## Abstract

Ets1 is a member of the Ets family of transcription factors. Ets1 is expressed in autoinhibited form and its DNA binding depends on partner proteins bound to adjacent sequences or the relative positioning of a second Ets-binding site (EBS). The autoinhibition of Ets1 is mediated by structural coupling of regions flanking the DNA-binding domain. The NMR structure of Ets1 revealed that the inhibitory regions comprised of helices HI1 and HI2 and H4 are packed together on the Ets domain to form an inhibitory module. The crystal structure of Ets1 unexpectedly revealed a homodimer in which homodimerisation occurs via swapping of HI1 helices. Modeling of DNA binding indicates that the Ets1 dimer can bind to two antiparallel pieces of DNA. To verify this, we crystallized and solved the structure of the complex comprised of Ets1 dimer and two pieces of DNA. DNA binding by Ets1 dimer resulted in formation of additional intermolecular protein•DNA interactions, implying that the complex formation is cooperative.

**Citation:** Babayeva ND, Baranovskaya OI, Tahirov TH (2012) Structural Basis of Ets1 Cooperative Binding to Widely Separated Sites on Promoter DNA. *PLoS ONE* 7(3): e33698. doi:10.1371/journal.pone.0033698

**Editor:** Sergey Korolev, Saint Louis University, United States of America

**Received:** January 19, 2012; **Accepted:** February 17, 2012; **Published:** March 14, 2012

**Copyright:** © 2012 Babayeva et al. This is an open-access article distributed under the terms of the Creative Commons Attribution License, which permits unrestricted use, distribution, and reproduction in any medium, provided the original author and source are credited.

**Funding:** This work was supported by National Institute of General Medical Sciences grant R01GM082923 and Nebraska Department of Health and Human Services grant LB506 to THT. This work was also based upon research conducted at the Northeastern Collaborative Access Team beamlines of the Advanced Photon Source, supported by award RR-15301 from the National Center for Research Resources at the National Institutes of Health. Use of the Advanced Photon Source is supported by the U.S. Department of Energy, Office of Basic Energy Sciences, under Contract No. DE-AC02-06CH11357. The funders had no role in study design, data collection and analysis, decision to publish, or preparation of the manuscript.

**Competing Interests:** The authors have declared that no competing interests exist.

\* E-mail: ttahirov@unmc.edu

## Introduction

Ets1, a founding member of the Ets (E-twenty-six-specific) family of transcription factors, was initially identified as the protooncogene corresponding to *v-ets* of the E26 leukemia virus [1,2]. Ets1 regulates expression of lymphocyte-specific genes [3], bone-specific genes [4], and genes involved in vascular development and angiogenesis [5]. Ets1 is amplified and rearranged in leukemia and lymphoma [6]. Elevated Ets1 expression has been observed in many invasive and metastatic solid tumors, including breast, lung, colon, pancreatic and thyroid cancer [6].

Ets family members contain a highly conserved DNA-binding Ets domain, an 85-amino acid winged helix-turn-helix DNA-binding domain which recognizes a core motif 5'-GGA(A/T)-3' referred to as Ets-binding site (EBS) [7,8]. The Ets proteins are often expressed in autoinhibited form and their DNA binding depends on partner proteins bound to adjacent sequences [9,10,11,12], including the relative positioning of a second EBS [13]. In the case of Ets1, autoinhibition is mediated by structural coupling of the regions flanking the DNA-binding domain. The NMR structure of the partially inhibited Ets1 fragment aa 301–441 shows that the inhibitory regions, which are folded as helices HI1 and HI2 N-terminal to the ETS domain and H4 C-terminal to the ETS domain, are packed together on the Ets domain to form an inhibitory module [14]. Deletion of either region or disruption of the inhibitory module by point mutations of Ets1 resulted in 10- to 20-fold increases in DNA-binding affinity [15,16,17,18,19]. Ets1 autoinhibition is counteracted by direct interaction of the DNA-binding domain and/or autoinhibitory

regions with regulatory partners, including Pax5 [11], Runx1 [20,21,22,23,24] and Runx2 [25,26], or by DNA-mediated homodimerization [27,28,29]. In the latter case, two Ets1 molecules were found to bind cooperatively to the palindromic sequences in which two head-to-head EBS were separated by four base pairs [27,28,29,30,31,32,33,34]. According to earlier studies, it is expected that upon DNA binding the inhibitory module of Ets1 is disrupted and the helix HI1 becomes disordered [35]. However, our study of Ets1 binding to palindromic EBS on stromelysin-1 promoter revealed that the structural integrity of the inhibitory module and its involvement in intermolecular interactions are essential for DNA-mediated homodimerization of Ets1 [36]. Because the regions flanking the Ets domain appear to fulfill dual and opposing roles such as autoinhibition and cooperative DNA binding, we revisited the interpretation of the role of Ets1 dimer formation which we observed in crystals (Tahirov, Inoue-Bungo and Ogata, PDB code 1gvj). Ets1 dimer with a similar overall conformation was observed in a different crystal form obtained in the Wolberger laboratory (PDB code 1mdo), to which they referred as a domain-swapped dimer [35]. Because Ets1 dimer retained its shape under different crystallization and crystal packing conditions, we looked at whether the dimerization may have any role in DNA binding. Modeling of DNA binding indicated that Ets1 dimer can bind to two antiparallel pieces of DNA. To verify Ets1 dimer binding to two separate pieces of DNA we crystallized and solved the structure of the complex comprised of Ets1 dimer and two pieces of DNA [referred to as (Ets1)<sub>2</sub>•2DNA]. The structure revealed that in spite of DNA binding the overall conformation of Ets1 dimer, including HI1 and

HI2, remains the same. These data shows that at high local concentration Ets1 homodimerization and cooperative DNA binding may have a regulatory role.

## Results

### Overall structure

Crystals belong to the monoclinic space group  $P2_1$  and diffract up to 3.1 Å resolution. The structure was solved by the molecular replacement method and refined to an  $R_{\text{free}}$  of 28.4%. The asymmetric unit contains two Ets1 molecules (residues 280–441) forming a dimer. The electron density is absent for the amino acid residues 280–301 and 438–441 of each Ets1 and these residues are excluded from the model. The DNA-binding areas of each Ets1 subunit are on the same side of the dimer and docked on two antiparallel pieces of dsDNA from TCR $\alpha$  promoter. Each Ets1 is bound to a separate piece of dsDNA resulting in formation of (Ets1) $_2$ •2DNA quaternary complex (Fig. 1).

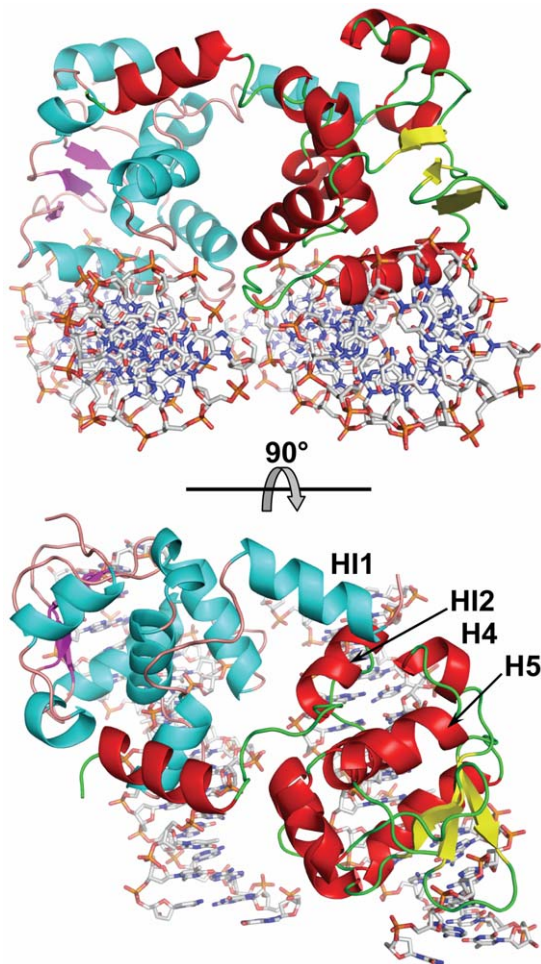


**Figure 1. Overall structure of (Ets1) $_2$ •2DNA.** Two orthogonal views are shown. Ets1 molecules are drawn as cartoons and DNA molecules are drawn as sticks. The helices, strands and coils are shown in cyan, magenta and light brown colors in one Ets1 molecule and respectively in red, yellow and green in another Ets1 molecule. The DNA molecules are colored by types of atoms: oxygen is red, nitrogen is blue, carbon is grey and phosphorus is orange. The labeled helices HI2, H4 and H5 are involved in docking of HI1 helix from another Ets1 subunit. doi:10.1371/journal.pone.0033698.g001

### Intermolecular interactions

Within the (Ets1) $_2$ •2DNA complex the Ets1•Ets1 interactions are observed at two equivalent positions (Fig. 1). They are similar to the intermolecular interactions found in the crystal structure of Ets1 dimer [35]. Briefly, at each position the interactions involve the N-terminal portion of HI1 helix from one subunit and H4 helix, a loop H4H5, HI2 helix and a loop HI1HI2 from another subunit (Fig. 1). The HI1 packs against the C-terminal of H4, making two main-chain to main-chain hydrogen bonds. The hydrogen bonds are also observed between the side chains of Lys305 and Tyr424 and between the carbonyl oxygen of Gly302 and hydroxyl oxygen of Tyr329. The small hydrophobic core is formed by packing the side chains of Phe304 and Tyr307 against a hydrophobic surface formed by Ile321, Pro322, Ala325, Leu326, Tyr329, Leu421 and Leu422.

The DNA binding by each Ets1 subunit is similar to that reported for Ets1•DNA complex [11]. However, within (Ets1) $_2$ •2DNA complex additional hydrogen bonds are observed between each Ets1 subunit and the neighboring DNA duplex. The potential hydrogen bonds involve the side chains of Asn380 and Lys383 from the loop H2H3 and DNA phosphate oxygen (Fig. 2). The positively charged surface of Ets1 facing the neighboring DNA (Fig. 3) also contributes to the overall stability of (Ets1) $_2$ •2DNA complex since the long-range electrostatic interactions enhance the DNA-binding affinity of the protein [37].

### Comparison with DNA-free Ets1 dimer

Superimposition of Ets1 dimers with and without DNA shows that DNA binding introduces only minor local changes in Ets1 dimer structure (Fig. 3A) with the root-mean-square deviations for the 271 matched  $\alpha$ -carbon atoms at 0.86 Å. The only notable difference is the disorder of the seven N-terminal residues within (Ets1) $_2$ •2DNA complex. In DNA-free Ets1 dimer the N-terminal residues are extended toward the protein's DNA backbone-binding surface and form two additional intermolecular hydrogen bonds at each site, His298 ND1...Ser 420 O and Lys299 NZ...Tyr329 O. The direction of the residues N-terminal to HI1 indicates that the extended N-terminal would mask the DNA backbone-binding surface of Ets1 (Fig. 3B). This is consistent with the autoinhibitory role of the residues N-terminal to HI1.

### Comparison with cooperative binding to palindromic EBS

Structural studies of two Ets1 bound to palindromic EBS on stromelysin-1 promoter [further referred to as (Ets1) $_2$ •DNA complex] revealed two areas of intermolecular interactions that are essential for cooperative DNA binding, and both areas contributed to the stability of the inhibitory module [36]. Interestingly, the loop H2H3 harboring Asn380 and Lys383 appears to play an important role in intermolecular interactions in both the (Ets1) $_2$ •2DNA and (Ets1) $_2$ •DNA complex structures. In the former structure it interacts with the backbone of DNA that is docked to the second Ets1 subunit (Fig. 2A), and in the latter structure it interacts with loop HI2HI1 of the second subunit (Fig. 2B). In the case of (Ets1) $_2$ •DNA complex the mutation of Asn380 to alanine resulted in the loss of cooperative DNA binding and in a reduction of activity at stimulating the stromelysin-1 promoter.

### Inhibitory module

Another common feature of Ets1 dimers found in crystal structures, including Ets1 dimer, (Ets1) $_2$ •DNA and (Ets1) $_2$ •2DNA, is conservation of the structure of inhibitory module comprised of

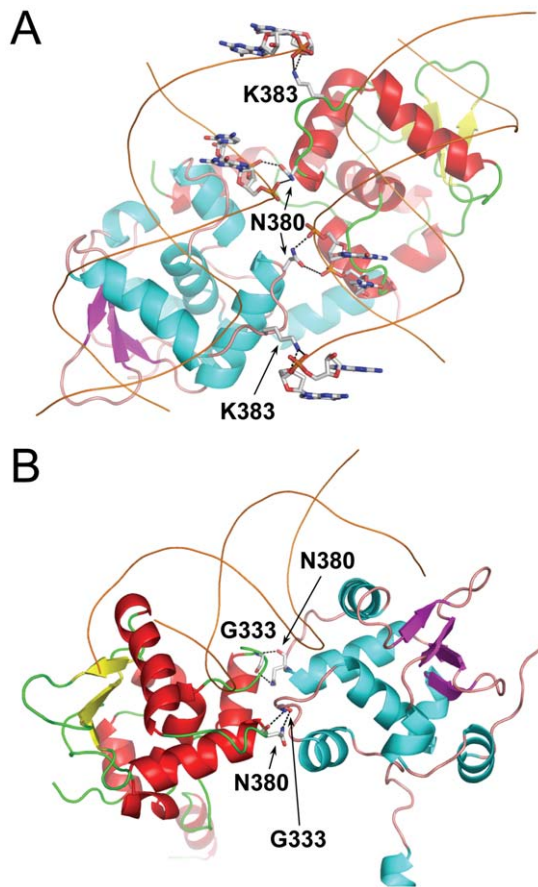


**Figure 2. Comparison of intermolecular hydrogen bonds in  $(Ets1)_2 \cdot 2DNA$  and  $(Ets1)_2 \cdot DNA$  complexes.** (A) Intermolecular hydrogen bonds between Ets1 and the neighboring DNA duplex within  $(Ets1)_2 \cdot 2DNA$  complex. (B) Intermolecular hydrogen bonds between Ets1 subunits in  $(Ets1)_2 \cdot DNA$  complex. In panels **A** and **B** Ets1 and DNA molecules are drawn as cartoons and interacting residues are drawn as sticks and labeled. The potential hydrogen bonds are shown as dotted lines. The color codes are as in Figure 1. doi:10.1371/journal.pone.0033698.g002

helices HI1, HI2 and H4, and the loops HI1HI2 and H4H5 (Fig. 1). Unlike these structures, DNA binding by monomeric Ets1 alone or in complex with a regulatory partner results in the disorder of helix HI1 [11,35]. Together, the DNA-free and DNA-bound crystal structures of Ets1 indicate that Ets1 autoinhibition could be counteracted by at least three different mechanisms: by disruption and disorder of autoinhibitory helix HI1 [35], by replacement of helix HI1 [36], and by direct competition with autoinhibitory sequences (Fig. 4). In all cases the end result is unmasking the DNA-binding surface of Ets1.

## Discussion

Interactions between transcriptional factors are often weak and transient, and are physiologically relevant only at high concentrations. It is possible that the weaker interactions prevent them from accidental aggregation. However, binding to adjacent sites on promoters and enhancers increases the local concentration of transcriptional factors dramatically, even if their concentration in the cell is very low [38]. An increase in local concentration also occurs for factors bound to widely separated sites on a promoter due to looping of promoter DNA [38,39,40]. Observation of the

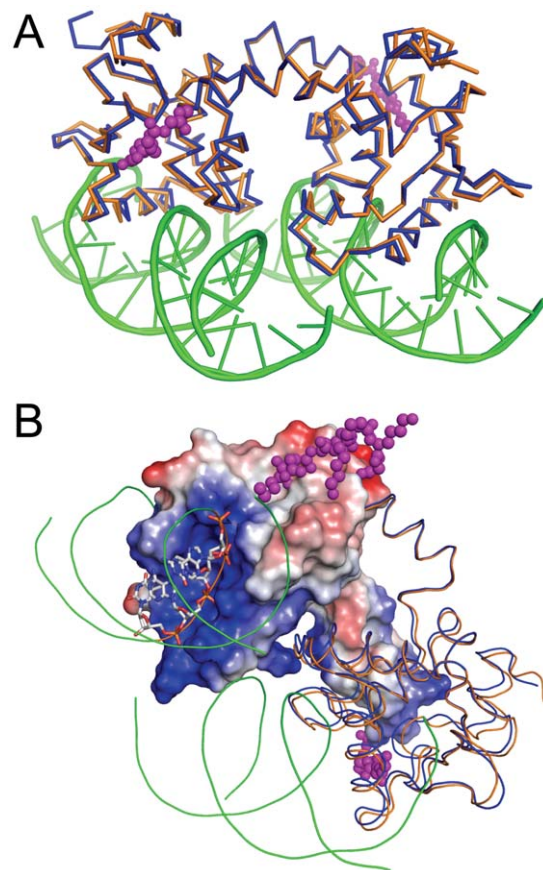


**Figure 3. Comparison of Ets1 dimers with and without DNA.** (A) Superimposition of DNA-free Ets1 dimer (blue) (PDB access code 1gvj) with DNA-bound Ets1 dimer (orange). (B) The molecules are superimposed and colored as in **A**. The charged surface is drawn for one of the Ets1 subunits in  $(Ets1)_2 \cdot 2DNA$  complex and the DNA residues docked to the surface of Ets1 are shown as sticks. The positively and negatively charged surface areas of Ets1 are in blue and red, respectively. In panels **A** and **B** the magenta balls highlight the atoms of the N-terminal residues of DNA-free Ets1 that are extended toward the DNA-binding surface of Ets1. doi:10.1371/journal.pone.0033698.g003

identical dimerization mode of Ets1 in crystals obtained under different conditions, with different truncated Ets1 constructs, and having different crystal packing, once again pointed to a tendency of Ets1 for dimerization at high concentrations. The Ets1 homodimer observed in the crystals might also form at a high local concentration of Ets1. Such a high local concentration would be achieved only if the Ets1 molecules bind to adjacent sites on DNA like in stromelysin-1 promoter [36] or to sites that are widely separated in sequence but closely positioned in space because of DNA looping. To test this hypothesis, we crystallized and solved the crystal structure of Ets1 homodimer bound to two separate dsDNA fragments. The structure revealed that Ets1 homodimer binds to parallel pieces of dsDNA having EBS with opposite orientation. The structure also revealed that Ets1 homodimer readily recognizes two antiparallel pieces of dsDNA without changing the conformation of DNA-binding domains and inhibitory helices.

It is not known whether Ets1 homodimer alone can support DNA looping or whether the function of other DNA-bending factors is necessary. However, Ets1 was shown to be capable of binding to nucleosomal DNA with the same order of affinity as



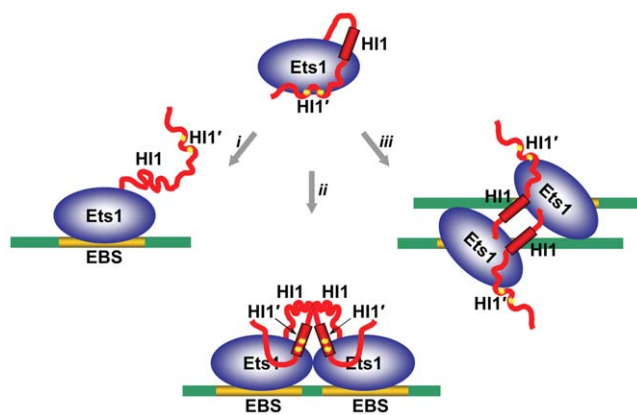


**Figure 4. Mechanisms of releasing the Ets1 autoinhibition upon DNA binding.** Three possible models of counteracting the autoinhibition: (i) by disruption of autoinhibitory helix HI1 interactions and its disorder upon binding to a single EBS [35], (ii) by replacement of helix HI1 by induced helix HI1' upon binding to a palindromic EBS [36], (iii) and by direct competition with autoinhibitory sequences upon binding to widely separated EBSs (this report). doi:10.1371/journal.pone.0033698.g004

that of binding to naked DNA [41]. Among the well characterized examples are Ets1 binding to nucleosomal DNA of HIV-1 long terminal repeat [42], platelet factor 4 [41] and immunoglobulin  $\mu$  heavy chain [43] enhancers. That is why it is interesting whether Ets1 is predisposed for binding to nucleosomal DNA also as a homodimer. Indeed, the separation of DNA fragments and exposed major groove positions of nucleosomal DNA coincide with Ets1-binding sites in  $(Ets1)_2 \cdot 2DNA$ . Figure 5A shows that Ets1 homodimer could be readily docked to nucleosomal DNA with only minor adjustments in Ets1 homodimer and nucleosomal DNA structures required for a tight complex formation.

Finally, we speculate that based on the  $(Ets1)_2 \cdot 2DNA$  complex structure two models of Ets1 cooperative binding to widely separated EBS are possible: cooperation via DNA looping (Fig. 5B) and cooperation on nucleosome core particles (Fig. 5C). Such cooperative binding would give an advantage to Ets1 for competing with other Ets family members both by dimerization and by making additional interactions with backbone phosphates and bases of DNA fragments harboring a second subunit of Ets1 dimer.

## Materials and Methods

### Preparation of $(Ets1)_2 \cdot 2DNA$

Ets1<sub>280–441</sub> has been cloned, expressed and purified according to reported protocols [36]. A double-strand oligonucleotide containing Runx1 and Ets1-binding region of TCR- $\alpha$  promoter was prepared by annealing synthetic oligonucleotides 5'-GGAAGCCA-CATCCTCT-3' and 5'-CAGAGGATGTGGCTTC-3' synthesized by the Eppley Molecular Core laboratory of University of Nebraska Medical Center. Each oligonucleotide was dissolved in 10 mM Tris•HCl (pH 7.5), 1 mM EDTA and 1 M NaCl at a concentration of 0.2 mM. Oligonucleotide pairs were annealed by heating to 95°C for 5 min and gradually cooling to room temperature over 3 h by using a PCR thermal cycler. The annealed DNA was desalted, dried and dissolved in 10 mM Tris•HCl (pH 8.0). Ets1<sub>280–441</sub> and the TCR $\alpha$  dsDNA were mixed in 1:1.05 ratio, incubated at room temperature for 20 min in 5 mM Tris•HCl buffer with pH 7.5 and 5 mM DTT and concentrated to 8.5 mg•ml<sup>-1</sup>. Complex formation was monitored by electrophoresis

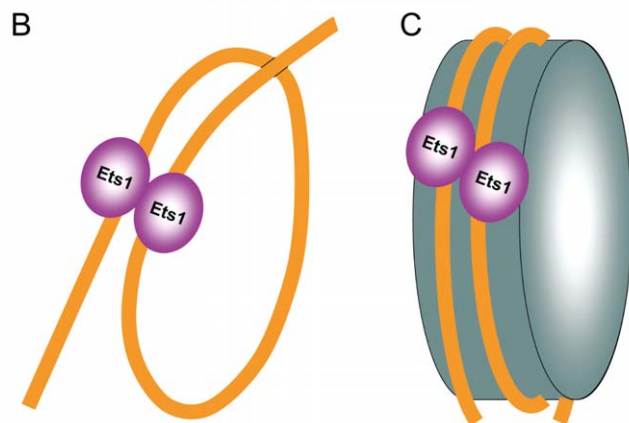
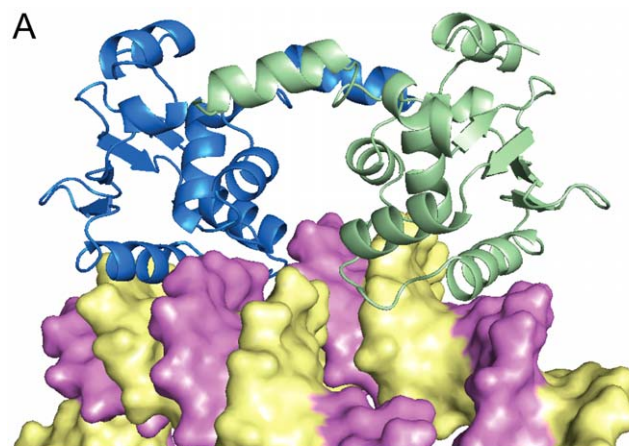


**Figure 5. Models of Ets1 binding to widely separated EBS.** (A) Docking of Ets1 homodimer to nucleosomal DNA based on the superimposition of DNA in the  $(Ets1)_2 \cdot 2DNA$  structure and the high-resolution structure of a nucleosome core particle (PDB access code 1kx5) [49]. Ets1 molecules are displayed as blue and green cartoons and DNA is displayed as a surface with the strands highlighted in yellow and magenta colors. (B) and (C) Schematic representation of two models of Ets1 cooperative binding to widely separated EBS on promoter DNA: (B) binding via looping of promoter DNA and (C) binding to a nucleosome core particle. doi:10.1371/journal.pone.0033698.g005

to confirm that the excess of DNA is approximately 5%. The complex containing solutions were stored in small aliquots at 253 K and each aliquot thawed only once before crystallization.

### Crystallization of $(Ets1)_2 \cdot 2DNA$ and diffraction data collection

Crystallization screening was performed using Natrix screen kit (Hampton Research) by the sitting-drop vapor-diffusion method at 295 K by mixing 1  $\mu$ l protein•DNA solution with 1  $\mu$ l reservoir solution. The rectangular thin plate crystals appeared in the 47<sup>th</sup> and 48<sup>th</sup> conditions of the Natrix screen kit. The optimizations of crystal growth conditions were performed with variation of additives, polyethylene glycols and the concentration of components. Thicker diffraction-quality plate crystals growing in aggregates were obtained at 295 K in 200 mM ammonium chloride, 10 mM calcium chloride, 50 mM Tris-HCl buffer (pH 8.5), 21% v/v polyethylene glycol monomethyl ether 2000 (PEG MME 2000) and 3% v/v glycerol. The best-shaped crystals were surgically separated from aggregates using microtools, washed four times and used for macroseeding in the drops of mother liquor equilibrated against the reservoir solution

**Table 1.** Data collection and refinement statistics.

Data collection	
Space group	$P2_1$
Cell dimensions:	
a (Å)	50.18
b (Å)	98.12
c (Å)	53.58
$\beta$ (°)	109.67
Resolution (Å)*	30-3.0 (3.11-3)
Unique reflections	9369
$R_{\text{merge}}$ (%)*	8.0 (36.3)
$I/\sigma(I)$	12 (2.2)
Completeness (%)	94.7 (87.9)
Redundancy	2.6 (1.9)
Temperature (K)	100
Mosaicity (°)	0.7–1.3
Refinement	
Resolution (Å)	30-3.1
No. reflections	8427
$R_{\text{work}}/R_{\text{free}}$	0.23/0.284
No. atoms/B-factors (Å <sup>2</sup> )	
Protein	2236/54.0
DNA	1300/43.3
Water	33/21.7
R.m.s. deviations	
Bond lengths (Å)	0.008
Bond angles (°)	1.3
Ramachandran plot	
Favored (%)	87.0
Allowed (%)	12.2
Generously allowed (%)	0.8

\*Values in parentheses are for the last shell.  
doi:10.1371/journal.pone.0033698.t001

containing 18.5% v/v of PEG MME 2000 instead of 21% v/v for 1 day. For X-ray diffraction data collection the crystals were soaked in cryoprotectant and mounted in nylon-fiber loops and flash-cooled in a dry nitrogen stream at 100 K. Cryoprotectant was prepared by the

## References

- Leprince D, Gégonne A, Coll J, de Taisne C, Schneberger A, et al. (1983) A putative second cell-derived oncogene of the avian leukaemia retrovirus E26. *Nature* 306: 395–397.
- Numm MF, Seeburg PH, Moscovici C, Duesberg PH (1983) Tripartite structure of the avian erythroblastosis virus E26 transforming gene. *Nature* 306: 391–395.
- Chen JH (1985) The proto-oncogene c-ets is preferentially expressed in lymphoid cells. *Mol Cell Biol* 5: 2993–3000.
- Raouf A, Seth A (2000) Ets transcription factors and targets in osteogenesis. *Oncogene* 19: 6455–6463.
- Sato Y (2001) Role of ETS family transcription factors in vascular development and angiogenesis. *Cell Struct Funct* 26: 19–24.
- Seth A, Watson DK (2005) ETS transcription factors and their emerging roles in human cancer. *Eur J Cancer* 41: 2462–2478.
- Donaldson LW, Petersen JM, Graves BJ, McIntosh LP (1994) Secondary structure of the ETS domain places murine Ets-1 in the superfamily of winged helix-turn-helix DNA-binding proteins. *Biochemistry* 33: 13509–13516.
- Nye JA, Petersen JM, Gunther CV, Jonsen MD, Graves BJ (1992) Interaction of murine ets-1 with GGA-binding sites establishes the ETS domain as a new DNA-binding motif. *Genes Dev* 6: 975–990.
- Mo Y, Ho W, Johnston K, Marmorstein R (2001) Crystal structure of a ternary SAP-1/SRF/c-fos SRE DNA complex. *J Mol Biol* 314: 495–506.
- Escalante CR, Brass AL, Pongubala JM, Shatova E, Shen L, et al. (2002) Crystal structure of PU.1/IRF-4/DNA ternary complex. *Mol Cell* 10: 1097–1105.
- Garvie CW, Hagman J, Wolberger C (2001) Structural studies of Ets-1/Pax5 complex formation on DNA. *Mol Cell* 8: 1267–1276.
- Janknecht R, Nordheim A (1993) Gene regulation by Ets proteins. *Biochim Biophys Acta* 1155: 346–356.
- Hodge DR, Robinson L, Watson D, Lautenberger J, Zhang XK, et al. (1996) Interaction of ETS-1 and ERG/FLI-1 proteins with DNA is modulated by spacing between multiple binding sites as well as phosphorylation. *Oncogene* 12: 11–18.
- Lee GM, Donaldson LW, Pufall MA, Kang HS, Pot I, et al. (2005) The structural and dynamic basis of Ets-1 DNA binding autoinhibition. *J Biol Chem* 280: 7088–7099.

addition 12% v/v of PEG 400 to a reservoir solution. Preliminary X-ray examinations of crystals were carried out using Rigaku R-AXIS IV imaging plate with Osmic VariMax<sup>TM</sup> HR mirror-focused Cu K<sub>α</sub> radiation from Rigaku FR-E rotating-anode generator operated at 45 kV and 45 mA. The final data set was collected on Argonne National Laboratory Advanced Photon Source beamline 24ID-C using an ADSC Q315 detector. All intensity data were indexed, integrated and scaled with DENZO and SCALEPACK from the HKL2000 program package [44]. The crystals belong to the monoclinic space group  $P2_1$  and diffract up to 2.8 Å resolution; however, the diffraction beyond 3.1 Å is anisotropic and the spots are too wide and elongated. The crystal parameters and data-processing statistics are summarized in Table 1. Unlike the (Ets1)<sub>2</sub>•2DNA crystals, the crystals of Ets1 dimer (PDB code 1gvj) were grown in the 9<sup>th</sup> condition of Hampton Research Crystal Screen kit and belong to a triclinic  $P1$  space group.

## (Ets1)<sub>2</sub>•2DNA structure determination

The structure was determined by the molecular replacement method starting with the coordinates of Ets1 (PDB entry 1gvj with an  $R_{\text{cryst}}$  of 20.8% and an  $R_{\text{free}}$  of 23.5% at 1.53 Å resolution). The asymmetric unit contained Ets1 homodimer and two pieces of dsDNA. The major manual rebuilding of the initial model was performed with TURBO-FRODO software. The refinement at 3 Å resolution resulted in a significant 25% jump of R-free for the reflections in the 3.1–3.0 Å shell. That is why the model was refined at 3.1 Å resolution to an  $R_{\text{cryst}}$  of 22.5% and an  $R_{\text{free}}$  of 28.3%. CNS version 1.1 [45] was used for all crystallographic computing. Application of zonal scaling [46] and bulk solvent correction improved the quality of electron density maps. The final refinement statistics are provided in Table 1. The figures containing molecular structures were drawn with PyMOL. The electrostatic surface potential was calculated and displayed with PyMOL [47]. Similar surface charge distribution was obtained also with GRASP [48].

## Accession numbers

Atomic coordinates and structure factors of (Ets1)<sub>2</sub>•2DNA have been deposited in the Protein Data Bank with accession number 3ri4.

## Author Contributions

Conceived and designed the experiments: THT. Performed the experiments: NDB OIB. Analyzed the data: NDB OIB THT. Wrote the paper: NDB THT.

15. Hagman J, Grosschedl R (1992) An inhibitory carboxyl-terminal domain in Ets-1 and Ets-2 mediates differential binding of ETS family factors to promoter sequences of the mb-1 gene. *Proc Natl Acad Sci U S A* 89: 8889–8893.
16. Jonsen MD, Petersen JM, Xu QP, Graves BJ (1996) Characterization of the cooperative function of inhibitory sequences in Ets-1. *Mol Cell Biol* 16: 2065–2073.
17. Lim F, Kraut N, Framptom J, Graf T (1992) DNA binding by c-Ets-1, but not v-Ets, is repressed by an intramolecular mechanism. *Embo J* 11: 643–652.
18. Petersen JM, Skalicky JJ, Donaldson LW, McIntosh LP, Alber T, et al. (1995) Modulation of transcription factor Ets-1 DNA binding: DNA-induced unfolding of an alpha helix. *Science* 269: 1866–1869.
19. Wasylyk C, Kerckaert JP, Wasylyk B (1992) A novel modulator domain of Ets transcription factors. *Genes Dev* 6: 965–974.
20. Wotton D, Ghysdael J, Wang S, Speck NA, Owen MJ (1994) Cooperative binding of Ets-1 and core binding factor to DNA. *Mol Cell Biol* 14: 840–850.
21. Sun W, Graves BJ, Speck NA (1995) Transactivation of the Moloney murine leukemia virus and T-cell receptor beta-chain enhancers by cbf and ets requires intact binding sites for both proteins. *J Virol* 69: 4941–4949.
22. Gu TL, Goetz TL, Graves BJ, Speck NA (2000) Auto-inhibition and partner proteins, core-binding factor beta (CBFbeta) and Ets-1, modulate DNA binding by CBFalpha2 (AML1). *Mol Cell Biol* 20: 91–103.
23. Goetz TL, Gu TL, Speck NA, Graves BJ (2000) Auto-inhibition of Ets-1 is counteracted by DNA binding cooperativity with core-binding factor alpha2. *Mol Cell Biol* 20: 81–90.
24. Kim WY, Sieweke M, Ogawa E, Wee HJ, Englmeier U, et al. (1999) Mutual activation of Ets-1 and AML1 DNA binding by direct interaction of their autoinhibitory domains. *Embo J* 18: 1609–1620.
25. Wai PY, Mi Z, Gao C, Guo H, Marroquin C, et al. (2006) Ets-1 and runx2 regulate transcription of a metastatic gene, osteopontin, in murine colorectal cancer cells. *J Biol Chem* 281: 18973–18982.
26. Sato M, Morii E, Komori T, Kawahata H, Sugimoto M, et al. (1998) Transcriptional regulation of osteopontin gene in vivo by PEBP2alphaA/CBFA1 and ETS1 in the skeletal tissues. *Oncogene* 17: 1517–1525.
27. Venanzoni MC, Robinson LR, Hodge DR, Kola I, Seth A (1996) ETS1 and ETS2 in p53 regulation: spatial separation of ETS binding sites (EBS) modulate protein: DNA interaction. *Oncogene* 12: 1199–1204.
28. Wasylyk C, Gutman A, Nicholson R, Wasylyk B (1991) The c-Ets oncoprotein activates the stromelysin promoter through the same elements as several non-nuclear oncoproteins. *Embo J* 10: 1127–1134.
29. Baillat D, Begue A, Stehelin D, Aumercier M (2002) ETS-1 transcription factor binds cooperatively to the palindromic head to head ETS-binding sites of the stromelysin-1 promoter by counteracting autoinhibition. *J Biol Chem* 277: 29386–29398.
30. Buttice G, Kurkinen M (1993) A polyomavirus enhancer A-binding protein-3 site and Ets-2 protein have a major role in the 12-O-tetradecanoylphorbol-13-acetate response of the human stromelysin gene. *J Biol Chem* 268: 7196–7204.
31. Basyiaux JP, Ferreira E, Stehelin D, Buttice G (1997) The Ets transcription factors interact with each other and with the c-Fos/c-Jun complex via distinct protein domains in a DNA-dependent and -independent manner. *J Biol Chem* 272: 26188–26195.
32. Tuck SP, Crawford L (1989) Characterization of the human p53 gene promoter. *Mol Cell Biol* 9: 2163–2172.
33. Baillat D, Leprivier G, Regnier D, Vintonenko N, Begue A, et al. (2006) Stromelysin-1 expression is activated in vivo by Ets-1 through palindromic head-to-head Ets binding sites present in the promoter. *Oncogene* 25: 5764–5776.
34. Reisman D, Eaton E, McMillin D, Doudican NA, Boggs K (2001) Cloning and characterization of murine p53 upstream sequences reveals additional positive transcriptional regulatory elements. *Gene* 274: 129–137.
35. Garvie CW, Pufall MA, Graves BJ, Wolberger C (2002) Structural analysis of the autoinhibition of Ets-1 and its role in protein partnerships. *J Biol Chem* 277: 45529–45536.
36. Babayeva ND, Wilder PJ, Shiina M, Mino K, Desler M, et al. (2010) Structural basis of Ets1 cooperative binding to palindromic sequences on stromelysin-1 promoter DNA. *Cell Cycle* 9: 3054–3062.
37. Tahirov TH, Sato K, Ichikawa-Iwata E, Sasaki M, Inoue-Bungo T, et al. (2002) Mechanism of c-Myb-C/EBP beta cooperation from separated sites on a promoter. *Cell* 108: 57–70.
38. Droge P, Muller-Hill B (2001) High local protein concentrations at promoters: strategies in prokaryotic and eukaryotic cells. *Bioessays* 23: 179–183.
39. Schleif R (1992) DNA looping. *Annu Rev Biochem* 61: 199–223.
40. Ogata K, Sato K, Tahirov TH (2003) Eukaryotic transcriptional regulatory complexes: cooperativity from near and afar. *Curr Opin Struct Biol* 13: 40–48.
41. Lu J, Pazin MJ, Ravid K (2004) Properties of ets-1 binding to chromatin and its effect on platelet factor 4 gene expression. *Mol Cell Biol* 24: 428–441.
42. Steger DJ, Workman JL (1997) Stable co-occupancy of transcription factors and histones at the HIV-1 enhancer. *Embo J* 16: 2463–2472.
43. Nikolajczyk BS, Sanchez JA, Sen R (1999) ETS protein-dependent accessibility changes at the immunoglobulin mu heavy chain enhancer. *Immunity* 11: 11–20.
44. Minor W, Cymborowski M, Otwinowski Z, Chruszcz M (2006) HKL-3000: the integration of data reduction and structure solution—from diffraction images to an initial model in minutes. *Acta Crystallogr D Biol Crystallogr* 62: 859–866.
45. Brünger AT, Clore GM, DeLano WL, Gros P, Grosse-Kunstleve RW, et al. (1998) Crystallography and NMR system ( CNS ): a new software system for macromolecular structure determination. *Acta Crystallogr Sect D* 54: 905–921.
46. Vassylyev DG, Vassylyeva MN, Perederina A, Tahirov TH, Artsimovitch I (2007) Structural basis for transcription elongation by bacterial RNA polymerase. *Nature* 448: 157–162.
47. PyMOL website. Available: <http://www.pymol.org>. Accessed 2012 Feb 21.
48. Nicholls A, Sharp KA, Honig B (1991) Protein folding and association: insights from the interfacial and thermodynamic properties of hydrocarbons. *Proteins* 11: 281–296.
49. Davey CA, Sargent DF, Luger K, Maeder AW, Richmond TJ (2002) Solvent mediated interactions in the structure of the nucleosome core particle at 1.9 Å resolution. *J Mol Biol* 319: 1097–1113.